

# Ex vivo biodistribution of gallium-68-labeled porous silicon nanoparticles

V K Tishchenko<sup>1</sup>, V. M. Petriev<sup>1,2</sup>, A A Mikhailovskaya<sup>1</sup>, O A Smoryzanova<sup>1</sup>,  
A V Kabashin<sup>2</sup> and I N Zavestovskaya<sup>2</sup>

<sup>1</sup> Tsyb Medical Radiological Research Centre, Obninsk, Russia

<sup>2</sup> National Research Nuclear University MEPhI (Moscow Engineering Physics Institute),  
Moscow, Russia

e-mail: petriev@mrrc.obninsk.ru

**Abstract.** The introduction of nanotechnology in nuclear imaging has gained significant interest and could have promising potential for clinical use. Tumor imaging with radiolabeled nanoparticles (NPs) may be used for early detection, characterization, staging of disease, and for monitoring treatment efficacy. In this study we evaluated the biodistribution of porous silicon NPs labeled with positron-emitter gallium-68 in Wistar rats with subcutaneously transplanted cholangioma RS-1. The uptake of <sup>68</sup>Ga-NPs in tumor tissue was 0.24±0.02 %ID/g at 5 min postinjection (p.i.) and climbed to 0.87±0.07 %ID/g at 5 h p.i. On the other hand, the amount of free <sup>68</sup>Ga injected as <sup>68</sup>GaCl<sub>3</sub> solution decreased from 0.34±0.07 %ID/g at 5 min p.i. to 0.07±0.01 %ID/g at 5 h p.i. The highest level of radioactivity revealed in liver (8.27–15.79 %ID/g), spleen (0.98–1.27 %ID/g), and lungs (0.98–1.80 %ID/g). <sup>68</sup>Ga-NPs were also determined in blood: up to 3.33±0.14 %ID/g at 5 min p.i. The uptake of <sup>68</sup>Ga-NPs in other organs and tissues didn't exceed 1 %ID/g. In conclusion, the obtained results suggest that <sup>68</sup>Ga-NPs could be suitable for use as molecular imaging probes.

## 1. Introduction

Nanotechnology is a rapidly expanding area of research with great potential in many sectors, especially in cancer medicine for tumor imaging. Nanoparticles (NPs) possess unique properties that distinguish them from bulk material: large functional surface area, easily controllable surface chemistry which facilitates binding to small molecule drugs, imaging labels and targeting ligands [1]. Molecular imaging using radiolabeled NPs has been widely applied due to its huge potential for early detection, accurate diagnosis, and treatment response in cancer. Positron emission tomography (PET), based on noninvasive imaging of tumor metabolism, can provide sensitive and specific approaches for targeted diagnosis of cancer.

Biomedical applications of porous silicon have been actively studied during the last 15 years, especially for drug delivery and imaging, due to excellent biocompatibility and biodegradability of porous silicon [2, 3]. It is degraded into silicic acid, which is a natural compound of the human body and can be cleared from the blood through the urine [4]. Moreover, Si-based nanomaterials can be used as active agents for cancer therapy due to their sensitizing properties under photo-, sono- and electromagnetic radio-frequency stimulus [5]. Also applications of porous silicon as drug carriers have been demonstrated [6].

Gallium-68 (<sup>68</sup>Ga) is a promising radionuclide for PET due to its excellent decay properties ( $T_{1/2} = 67.7$  min,  $\beta^+ = 89\%$ ,  $E_{\beta_{\max}} = 1.9$  MeV). Moreover, <sup>68</sup>Ga is available from the <sup>68</sup>Ge/<sup>68</sup>Ga-generator



system. The mother nuclide  $^{68}\text{Ge}$  has a half-life of 270.8 d, guaranteeing prolonged use of generator (~1 year). In order to combine the advantageous properties of PET and nanomaterials we labeled porous silicon NPs with  $^{68}\text{Ga}$  ( $^{68}\text{Ga}$ -NPs) and evaluated their biodistribution in tumor-bearing Wistar rats.

## 2. Methods and materials

All biodistribution studies were carried out in Wistar rats weighting 140-160 g and tumor xenografts of cholangioma RS-1. To obtain a solid form of cholangioma RS-1 the donor rat with tumor was killed by cervical disruption, then tumor tissue was isolated, ground up, diluted in physiological saline and implanted subcutaneously into right flanks of Wistar rats (100 mg/rat in a volume of 0.1 ml). When the tumor volume reached 0.7-0.8 cm<sup>3</sup>, the rats were intravenously injected with 0.37 MBq of  $^{68}\text{Ga}$ -NPs, or  $^{68}\text{GaCl}_3$  (n = 16 each tracer) in a volume of 0.1 ml. Animals were sacrificed at 5 min, 1, 3 and 5 h after injection. Four rats were used for each time points. The samples of tissues and organs were collected, weighed, and measured by automatic gamma counter. The amount of activity was presented as a percentage of the injected dose per gram of tissue (%ID/g). All the biodistribution studies were carried out in strict compliance with the national laws related to the conduct of animal experiments.

The results from the biodistribution data for each group of mice were expressed as mean value and standard error of the mean ( $M \pm m$ ). Student's *t* test was used to analyze data throughout all studies between groups at different time points, and  $p \leq 0.05$  was considered statistically significant.

## 3. Results and discussion

A comparative uptake of  $^{68}\text{Ga}$ -NPs and  $^{68}\text{GaCl}_3$  in tumor is shown in figure 1. The level of  $^{68}\text{Ga}$ -NPs in tumor tissue was  $0.24 \pm 0.02$  %ID/g at 5 min postinjection (p.i.) and climbed to  $0.57 \pm 0.01$ ,  $0.83 \pm 0.03$ , and  $0.87 \pm 0.07$  %ID/g at 1 h, 3 h, and 5 h p.i., respectively. On the other hand, the amount of free  $^{68}\text{Ga}$  injected as  $^{68}\text{GaCl}_3$  solution decreased from  $0.34 \pm 0.07$  %ID/g at 5 min p.i. to  $0.07 \pm 0.01$  %ID/g at 5 h p.i.

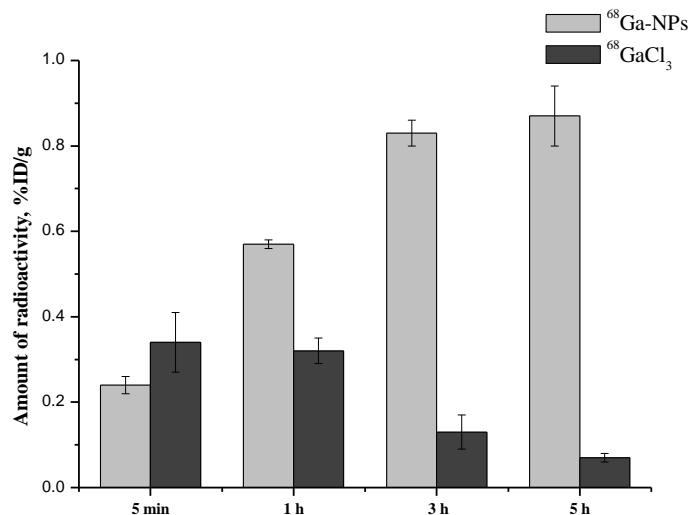


**Figure 1.** Specific amount of radioactivity in tumor after intravenous injection of  $^{68}\text{Ga}$ -NPs and  $^{68}\text{GaCl}_3$  (in %ID/g)

Well-designed NPs with an optimal size can accumulate in tumor tissue due to enhanced permeability and retention effect, which was first time described in work of Matsumura et al. [7]. Unlike normal vasculatures, tumor blood vessels usually have large pore openings (0.1–3  $\mu\text{m}$  in diameter). In addition, the amount of pericytes on tumor vessels is diminished as compared with

normal tissues [8]. These factors lead to significantly higher vascular permeability of tumor and allow the accumulation of NPs.

On the other hand, vascular hyperpermeability and impaired lymphatic drainage in tumor tissue result in elevated interstitial fluid pressure and limit NPs uptake. Dense stroma, consisting of fibroblasts, tumor-associated fibroblasts, epithelium, endothelium, muscle cells, and immune cells, is also a barrier to NPs extravasation [9]. Stroma cells compress intratumoral blood and lymphatic vessels, which consequently impairs blood flow, leading to blood stasis, loss of function, and further inhibition of NPs penetration [10]. It can explain sufficiently low amounts of  $^{68}\text{Ga}$ -NPs in tumor.

The major limitation of nanodiagnostic or therapeutic delivery is its inability to reach adequate levels of drugs in tumor due to nonspecific uptake of NPs in healthy organs. In our study the highest level of radioactivity revealed in organs of the reticuloendothelial system (RES): liver (8.27–15.79 %ID/g), spleen (0.98–1.27 %ID/g), and lungs (0.98–1.80 %ID/g), as shown in figure 2. RES consists of macrophages, which begin to adsorb NPs immediately after injection. This process starts with opsonization of NPs, involving the adsorption of plasma proteins, including serum albumin, apolipoproteins, complement components and immunoglobulins, onto the surface of circulating NPs [11]. Following protein adsorption, NPs undergo attachment to opsonin-recognizing specific receptors on the surface of phagocytes, after which NPs are internalized, transported to phagosomes and fused with lysosomes [12].

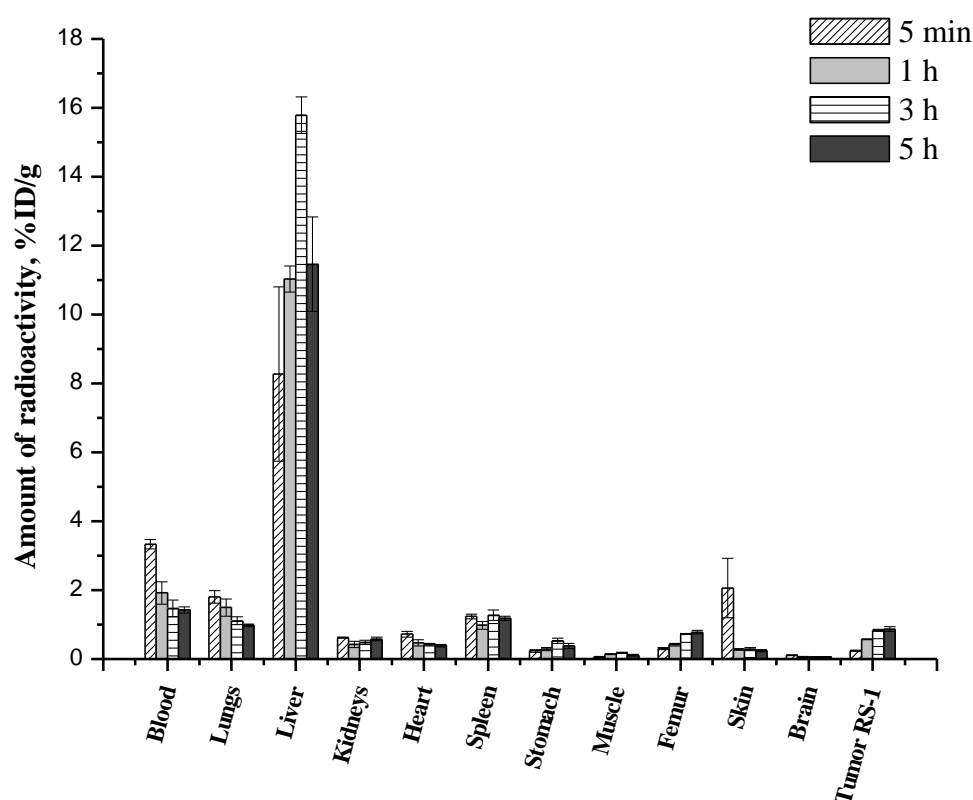


**Figure 2.** Specific amounts of radioactivity in organs and tissues in Wistar rats with cholangioma RS-1 at different time points after intravenous injection of  $^{68}\text{Ga}$ -NPs (%ID/g)

$^{68}\text{Ga}$ -NPs were also determined in blood: up to  $3.33 \pm 0.14$  %ID/g at 5 min p.i. Then  $^{68}\text{Ga}$ -NPs gradually decreased to  $1.43 \pm 0.09$  %ID/g at 5 h p.i.  $^{68}\text{GaCl}_3$  had the similar level of activity in blood: 0.78–3.64 %ID/g. The uptake of  $^{68}\text{Ga}$ -NPs in kidneys was significantly lower than that of free  $^{68}\text{Ga}$ . Thus, the accumulation of  $^{68}\text{Ga}$ -NPs fluctuated from  $0.43 \pm 0.09$  to  $0.62 \pm 0.02$  %ID/g, whereas the

uptake of  $^{68}\text{GaCl}_3$  decreased from  $3.57\pm 0.89$  at 5 min p.i. to  $2.05\pm 0.34$  %ID/g at 5 h p.i. Low uptake (less than 1 %ID/g) of  $^{68}\text{Ga}$ -NPs was observed in heart, stomach, muscle, and brain.

It is known that free  $^{68}\text{Ga}$  has high affinity to hydroxyapatite and cortical matrix of bone [13]. In our study the concentration of  $^{68}\text{GaCl}_3$  in femur reached  $3.03\pm 0.62$  %ID/g at 1 h p.i. The uptake of  $^{68}\text{Ga}$ -NPs in femur increased in time-dependent manner to  $0.78\pm 0.06$  %ID/g at 5 h p.i.

#### 4. Summary

The obtained results of  $^{68}\text{Ga}$ -NPs biodistribution revealed that the large part of injected activity accumulated in organs of the reticuloendothelial system: liver, spleen, and lungs. Tumor uptake of  $^{68}\text{Ga}$ -NPs was higher as compared with  $^{68}\text{GaCl}_3$  and increased gradually up to  $0.87\pm 0.07$  %ID/g. In conclusion, the obtained results suggest that  $^{68}\text{Ga}$ -NPs could be suitable for use as molecular imaging probes, but it is necessary to prolong blood circulation time of  $^{68}\text{Ga}$ -NPs by coating their surface with hydrophilic polymers, such as polyethylene glycol.

#### References

- [1] Goel S, England C E, Chen F and Cai W Positron emission tomography and nanotechnology: a dynamic duo for cancer theranostics 2016 *Adv. Drug Delivery Rev.* **42** 465–69
- [2] Low S P and Voelcker D N H 2014 Biocompatibility of porous silicon. In: *Canham L.T., editor. Handbook of Porous Silicon Springer International Publishing, Cham, Switzerland* 1–13
- [3] Shabir Q 2014 Biodegradability of porous silicon. In: *Canham L.T., editor. Handbook of Porous Silicon. Springer International Publishing, Cham, Switzerland* 395–401
- [4] Santos H A, Bimbo L M, Lehto V P, Airaksinen A J, Salonen J and Hirvonen J Multifunctional porous silicon for therapeutic drug delivery and imaging 2011 *Curr. Drug Discov. Technol.* **8**(3) 228–49
- [5] Tolstik E, Osminkina L A, Akimov D, Gongalsky M B, Kudryavtsev A A, Timoshenko V Y, Heintzmann R, Sivakov V and Popp J Linear and Non-Linear Optical Imaging of Cancer Cells with Silicon Nanoparticles 2016 *Int. J. Mol. Sci.* **17**(9) E1536
- [6] Salonen J, Kaukonen A M, Hirvonen J and Lehto V P Mesoporous silicon in drug delivery applications 2008 *J. Pharm. Sci.* **97**(2) 632–53
- [7] Matsumura Y and Maeda H A new concept for macromolecular therapeutics in cancer chemotherapy: mechanism of tumoritropic accumulation of proteins and the antitumor agent smancs 1986 *Cancer Res.* **46**(12 Pt 1) 6387–92
- [8] Cao Y, Zhang Z L, Zhou M, Elson P, Rini B, Aydin H, Feenstra K, Tan M H, Berghuis B, Tabbey R, Resau J H, Zhou F J, Teh B T and Qian C N Pericyte coverage of differentiated vessels inside tumor vasculature is an independent unfavorable prognostic factor for patients with clear cell renal cell carcinoma 2013 *Cancer* **119** 313–24
- [9] Duyverman A M, Steller E J, Fukumura D, Jain R K and Duda D G Studying primary tumor-associated fibroblast involvement in cancer metastasis in mice 2012 *Nat. Protoc.* **7** 756–62
- [10] Padera T P, Stoll B R, Tooredman J B, Capen D, di Tomaso E and Jain R K Pathology: cancer cells compress intratumour vessels 2004 *Nature* **427** 695
- [11] Tenzer S, Docter D, Kuharev J, Musyanovych A, Fetz V, Hecht R, Schlenk F, Fischer D, Kiouptsi K, Reinhardt C, Landfester K, Schild H, Maskos M, Knauer S K and Stauber R H Rapid formation of plasma protein corona critically affects nanoparticle pathophysiology 2013 *Nat. Nanotechnol.* **8**(10) 772–81
- [12] Sahay G, Alakhova D Y and Kabanov A V Endocytosis of nanomedicine 2010 *J. Control. Release* **145** 182–95
- [13] Toegel S, Wadsak W, Mien L K, Viernstein H, Kluger R, Eidherr H, Haeusler D, Kletter K, Dudczak R and Mitterhauser M Preparation and pre-vivo evaluation of no-carrier-added, carrier-added and cross-complexed [ $^{68}\text{Ga}$ ]-EDTMP formulations 2008 *Eur. J. Pharm. Biopharm.* **68** 406–12